

## SPATIAL HETEROGENEITY IN SIMPLE DETERMINISTIC SIR MODELS ASSESSED ECOLOGICALLY

E. K. WATERS<sup>✉1,2</sup>, H. S. SIDHU<sup>1</sup> and G. N. MERCER<sup>3</sup>

(Received 26 July, 2012; revised 2 October, 2012; first published online 9 April, 2013)

### Abstract

Patchy or divided populations can be important to infectious disease transmission. We first show that Lloyd's mean crowding index, an index of patchiness from ecology, appears as a term in simple deterministic epidemic models of the SIR type. Using these models, we demonstrate that the rate of movement between patches is crucial for epidemic dynamics. In particular, there is a relationship between epidemic final size and epidemic duration in patchy habitats: controlling inter-patch movement will reduce epidemic duration, but also final size. This suggests that a strategy of quarantining infected areas during the initial phases of a virulent epidemic might reduce epidemic duration, but leave the population vulnerable to future epidemics by inhibiting the development of herd immunity.

2010 *Mathematics subject classification*: 92B05.

*Keywords and phrases*: SIR model, ecology, infectious diseases, spatial dynamics.

### 1. Introduction

It is evident that just as sexual reproduction amongst animals is limited by the availability of sexual partners, whether due to spatial or behavioural reasons [21, 24], propagation of communicable diseases is limited by the availability of susceptible persons who can be infected by infectious individuals. At least in part, the supply of susceptible persons varies with space: spatial variability may either arise from, cause or merely reflect behavioural heterogeneity, though identifying which is the case can be difficult [9]. The simplest deterministic models of disease dynamics assume homogeneous mixing and are limited in their capacity to model spatial heterogeneity because homogeneous mixing assumes spatially as well as temporally uniform mixing.

<sup>1</sup>School of Physical, Environmental and Mathematical Sciences, The University of New South Wales Canberra, Australian Defence Force Academy, PO Box 7916, Canberra BC 2610, Australia; e-mail: [edward.waters.nsw@gmail.com](mailto:edward.waters.nsw@gmail.com), [h.sidhu@adfa.edu.au](mailto:h.sidhu@adfa.edu.au).

<sup>2</sup>University of Notre Dame Australia, PO Box 944, Broadway, NSW 2007, Australia.

<sup>3</sup>National Centre for Epidemiology and Population Health, The Australian National University, Canberra, ACT 0200, Australia; e-mail: [geoff.mercer@anu.edu.au](mailto:geoff.mercer@anu.edu.au).

© Australian Mathematical Society 2013, Serial-fee code 1446-1811/2013 \$16.00

Examples of infectious disease models assuming homogeneous mixing include the susceptible–infected–susceptible (SIS) framework, where individuals do not develop immunity to the infectious agent, and the susceptible–infected–recovered (SIR) framework, where recovered individuals are immune for life [1].

Whilst many epidemiological models have attempted to incorporate heterogeneity, this has most often been done by modelling heterogeneous behaviour by individuals rather than modelling space as a surrogate for behavioural heterogeneity or as the dominant factor influencing heterogeneity. Classic examples of models incorporating behavioural heterogeneity are age structured models with risk groups whose interactions are governed by mixing matrices [12]. Explicitly individual based models are the logical extension to this framework, as every individual might form their own risk group [25]. Some transmission models do include spatial variability in infection rather than modelling heterogeneity at the level of individuals or groups, but these more often deal with animal disease [5, 22]. In part this may reflect a greater emphasis on spatial heterogeneity as a surrogate measure or driver of behavioural or genetic heterogeneity in plant and animal sciences, especially in ecology.

A number of ways of assessing spatial heterogeneity are commonly used in ecological sampling studies, and one of these, Lloyd's index of mean concentration or mean demand ( $C^*$ ) [14, 18], can be expressed as a linear function of the mean number of individuals in a population [13], enabling it to be easily incorporated in deterministic epidemic and ecological models to model heterogeneity. Whilst  $C^*$  has been used in this way to account for spatial heterogeneity in the number of infected individuals in different areas when modelling sexually transmitted infections in animal and human populations [5, 26], the assumption that susceptible *as well as* infected individuals might be nonuniformly distributed in space has not been explicitly modelled. This paper uses  $C^*$  together with Lloyd's index of interspecific mean crowding,  $m_{xy}^*$  [18], and Iwao's index of spatial overlap,  $\gamma$  [10, 15], to explicitly model the effect of heterogeneous distributions of infected and susceptible individuals on the dynamics of a simple SIR model. To examine the implications of spatial heterogeneity for the management of specific disease types, two different types of infections are simulated in patchy environments: a short-lived respiratory disease and a long-lived sexually transmitted infection.

**1.1. Lloyd's interspecific mean crowding and mean concentration** The SIR model can be thought of as a predator–prey model where infected individuals prey on susceptible individuals with a 1:1 efficiency: every susceptible individual predated upon results in a 1:1 increase in the number of infected individuals. Lloyd's interspecific index of mean crowding,  $m_{xy}^*$ , measures the crowding of individuals of species  $y$  on species  $x$ , where crowding is defined as the extent to which the average number of individuals of species  $y$  per area outnumbers the average number of individuals of species  $x$  per area [18]. Assuming that  $y$  is a predator and  $x$  a prey species, the index can be used to examine how different average numbers of predators in discrete areas affect the dynamics of an SIR model [10]. Replacing  $x$  and  $y$  with  $S$

and  $I$ , the number of susceptible and infected individuals in a population,  $m_{IS}^*$  gives the average number of susceptible individuals per infected partner in a given area. The index  $m_{IS}^*$  is calculated over a population divided into  $q = 1, \dots, Q$  distinct patches as [18]

$$m_{IS}^* = \frac{\sum_{q=1}^Q S_q I_q}{\sum_{q=1}^Q I_q},$$

where  $S_q$  and  $I_q$  are the numbers of susceptibles and infectives in patch  $q$ . The reciprocal quantity, the mean number of infectives per susceptible individual per patch, is given by

$$m_{SI}^* = \frac{\sum_{q=1}^Q S_q I_q}{\sum_{q=1}^Q S_q}.$$

When there is a proportional relationship between  $S$  and  $I$ , we have  $m_{IS}^* = C_S^*$ , where  $C_S^*$  is the *mean concentration* of susceptibles [15]. The mean concentration of susceptibles is interpreted biologically as the average number of susceptible individuals per susceptible individual per patch [8, 15], and is given mathematically by the ratio of the first and second raw moments (mean and mean squared deviation about the origin) if  $S_q$  is a random variable [14, 18]. An analogous quantity, the mean concentration of infectives,  $C_I^*$ , can be arrived at by the same calculation. When the average number of infected individuals per patch is proportionally related to the number of susceptibles per patch,  $m_{IS}^* = C_I^*$  [15].

**1.2. Iwao's indices of spatial correlation** In 1977, Iwao [15] proposed several indices for summarizing the effects of changes in mean concentration and interspecific mean crowding on the spatial overlap between heterogeneously distributed organisms. In the context of susceptibles and infectives, Iwao's  $\gamma$  index takes a value of 1 when a proportional relationship exists between  $S$  and  $I$  and a value of 0 when no infectives share patches with susceptible individuals (exclusion) [10, 15]. In 1984, Fujita [10] used changes in  $\gamma$  to understand the contribution of spatial heterogeneity to oscillations in predator and prey populations, but  $\gamma$  has not previously been used to study the effect of spatial heterogeneity on the initial growth and peak size of epidemics. Iwao [15] defines  $\gamma$  as

$$\gamma = \sqrt{\frac{m_{SI}^* m_{IS}^*}{C_S^* C_I^*}},$$

where  $m_{SI}^*$ ,  $m_{IS}^*$ ,  $C_S^*$  and  $C_I^*$  are the interspecific mean crowding indices and mean concentrations of susceptibles and infectives (defined above). Let  $\gamma_i$  be the value of  $\gamma$  when the distributions of  $S$  and  $I$  are uncorrelated, which is given by

$$\gamma_i = \sqrt{\frac{\bar{S} \bar{I}}{C_S^* C_I^*}},$$

where  $\bar{S}$  and  $\bar{I}$  are the arithmetic mean numbers of susceptibles and infectives over all patches. Comparison of  $\gamma_i$  to  $\gamma$  can be used as to qualitatively assess the magnitude of any correlation in the spatial distributions of  $S$  and  $I$ .

Whilst comparison of  $\gamma_i$  to  $\gamma$  indicates the strength of any correlation, it cannot indicate whether the relationship between  $S$  and  $I$  is in the negative or positive direction. A negative relationship suggests a pattern of localized epidemics, whereas in an endemic infection infectives and susceptibles are positively spatially correlated. Iwao's index  $\omega$  can be used to evaluate the direction of the correlation between the distributions of  $S$  and  $I$ . Where  $\gamma \geq \gamma_i$ ,

$$\omega = \sqrt{\frac{m_{SI}^* m_{IS}^* - \bar{S} \bar{I}}{C_S^* C_I^* - \bar{S} \bar{I}}};$$

otherwise

$$\omega = \sqrt{\frac{m_{SI}^* m_{IS}^*}{\bar{S} \bar{I}}} - 1.$$

## 2. Accounting for spatial heterogeneity in an SIR model

In the basic SIR model, the change in the number of individuals in the susceptible, infectious and recovered states with respect to time  $t$ , assuming a constant population size  $N = S(t) + I(t) + R(t)$ , is given by [1]

$$\begin{aligned}\dot{S} &= \mu N - \mu S - \frac{\beta}{N} S I, \\ \dot{I} &= \frac{\beta}{N} S I - \alpha I - \mu I, \\ \dot{R} &= \alpha I - \mu R,\end{aligned}$$

where  $\alpha$  is the recovery rate,  $\mu$  is the birth and death rate and  $\beta S I / N$  describes the transmission process. Substituting  $R(t) = N - I(t) - S(t)$  eliminates the equation for recovered, yielding

$$\begin{aligned}\dot{S} &= \mu N - \mu S - \frac{\beta}{N} S I, \\ \dot{I} &= \frac{\beta}{N} S I - \alpha I - \mu I.\end{aligned}\tag{2.1}$$

Dividing the population in (2.1) into  $Q$  patches, rewrite (2.1) as

$$\begin{aligned}\dot{S} &= \sum_{q=1}^Q \left( \mu N_q - \mu S_q - \frac{\beta}{N_q} S_q I_q \right), \\ \dot{I} &= \sum_{q=1}^Q \left( \frac{\beta}{N_q} S_q I_q - \alpha I_q - \mu I_q \right),\end{aligned}$$

and divide through by  $\sum_{q=1}^Q I_q$ , giving

$$\begin{aligned} \frac{1}{\sum_{q=1}^Q I_q} \dot{S} &= \frac{\sum_{q=1}^Q (\mu N_q - \mu S_q - (\beta/N_q) S_q I_q)}{\sum_{q=1}^Q I_q} \\ \frac{1}{\sum_{q=1}^Q I_q} \dot{I} &= \frac{\sum_{q=1}^Q ((\beta/N_q) S_q I_q)}{\sum_{q=1}^Q I_q} - \alpha - \mu. \end{aligned} \quad (2.2)$$

Note that  $\sum_{q=1}^Q S_q I_q / \sum_{q=1}^Q I_q$  is equal to the mean crowding coefficient of  $S$  on  $I$ , namely  $m_{IS}^*$ . The maximum number of patches that the population can be divided into is equal to the number of individuals in the population, which turns the model into an agent based model. If the number of patches takes on this maximum value ( $Q = N$ ) then this relates back to the original SIR variables as  $\sum_{q=1}^Q S_q = S$ ,  $\sum_{q=1}^Q I_q = I$  and  $\sum_{q=1}^Q N_q = N$ . In the special case of homogeneous mixing ( $N_q$ ,  $S_q$  and  $I_q$  equal in all patches), when  $Q = N$  the agent based model can be perfectly described by the homogeneous-mixing deterministic SIR model (2.1).

It is clear that Lloyd's interspecific mean crowding subsists within a basic SIR model divided into patches. Therefore, analysis of interspecific mean crowding using Lloyd's index and Iwao's  $\gamma$  can be used to investigate changes in the spatial correlation as an epidemic progresses [10, 15]. In the uniform or infection-free case, the relation between  $S$  and  $I$  is constant and proportional, and thus  $\gamma = 1$  at all times. The value of the index  $\omega$  would also remain constant over time, but  $\omega$  could take on different values between  $-1$  and  $1$  based on the ratio of  $S$  or  $I$ , taking a value closer to  $0$  as this ratio approaches unity.

### 3. Examples of a patchy SIR model

**3.1. General characteristics** In nature, populations are often divided into discontinuous patches, which are connected by the movement of individuals from patch to patch [17]. Phenomenological models of such patchy populations capture the most important characteristics of these systems (autonomous processes within patches linked by inter-patch movement) in the simplest form possible. The circular stepping stone model of Maruyama [20] for a population divided into  $Q = 12$  patches is depicted in Figure 1. The model allows bidirectional movement (hereafter referred to as migration) of randomly selected individuals to adjacent patches. More traditional models of epidemics in patchy environments might divide the population into discrete, square patches arranged in a grid, where migration occurs in both directions across each edge bordering an adjoining patch [6]. Both the grid and circular stepping stone approaches share some disadvantages and unrealistic assumptions. Namely, they neither realistically represent the nature of patches in a heterogeneous population, which are unlikely to be uniform in size or equidistant, nor do they attempt to realistically model migration between patches, which will certainly not occur either at random or at a constant rate in nature, regardless of the spatial scale used.

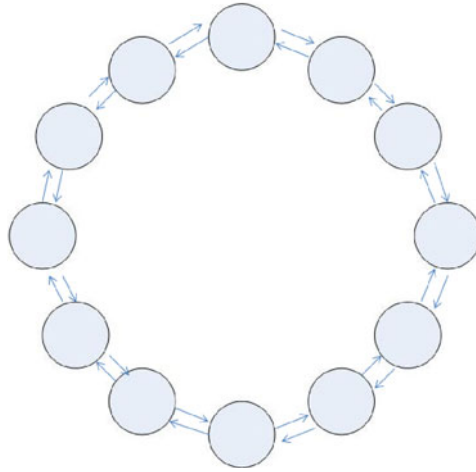


FIGURE 1. The circular stepping stone multi-patch model of Maruyama [20]. Movement between patches is bidirectional and patches are assumed to be equidistant. A similar form was used by Fujita [10].

Given these shared disadvantages, the Maruyama circular model has advantages as a phenomenological model over square grids. Firstly, it avoids edge effects, where square patches on the edge of the grid connect to fewer patches than those in the centre and thus have different dynamics. Secondly, the lack of edges or boundaries within the circle creates an elegant but simple model of a metapopulation that is itself unique and characterized by common features, but has diversity within its patches. As such it is a good phenomenological model for many cities and towns, which might have common features overall and yet have discrete patches within notably different characteristics.

In the circular model of a patchy population, two different types of epidemics (long and short duration) whose dynamics are described by (2.2) were simulated. These simulations were written in the R programming language [23], and utilized a time step of 1 day. For each type of infection, three different sets of initial and epidemic conditions were examined. To obtain the homogeneous model as a reference case, each patch initially contained 5000 individuals, of whom one was infected. The population size of 5000 was chosen because it was sufficiently large to allow the deterministic nature of the system to predominate. In the most realistic model, the number of infected individuals and the total population size in each patch at initialization were randomly selected (Poisson distributed with a mean of 1), and one individual per day per patch was allowed to migrate to an adjacent patch over the entire course of the simulation. The migrating individual was chosen randomly so that migration was independent of disease status. Because individuals migrate to and from patches at the same rate, migration terms in each direction cancel, so no additional terms need to be added to (2.2).

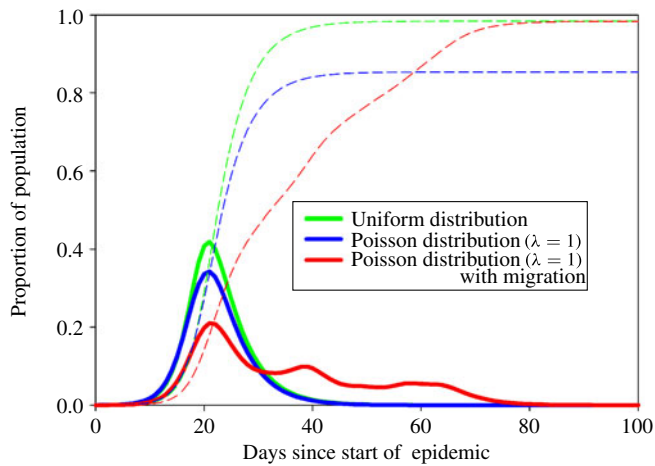


FIGURE 2. The proportion of the population infected (solid line) and recovered (dashed line) under three different scenarios: uniform distribution (total population size, proportion infected and recovered uniform in each patch, green lines); Poisson distributed initial population size and proportion infected per patch (blue lines); and Poisson distributed in a similar fashion, but with inter-patch migration at a rate of one randomly selected individual per day (red lines). (Colour available online.)

The initial distribution of infected individuals was chosen as it resulted in some disease-free patches, but most patches having one infected individual (similar to the uniform case). For comparison, an epidemic with the same initial conditions, but without the movement of individuals between patches, was examined. This latter case most closely replicates a scenario where the distance between discontinuous patches is so great that little interaction takes place, but also sheds light on the possible effects of quarantining, though it may overestimate the intensity of such effects by limiting the movement of noninfectious individuals and by stopping migration at epidemic commencement rather than when a detectable level of infection is reached.

**3.2. Example 1: a short-lived respiratory infection** First, an epidemic of a virulent respiratory illness (average basic reproductive number  $R_0$  of 3.75 and duration of infection of 6 days as in the British Boarding School 1978 H1N1 outbreak [2]) was simulated over a 100-day period. The results for a uniform distribution and heterogeneous distributions with and without migration are shown in Figure 2. When patches are not homogeneous, the rate at which the epidemic peak is reached is not affected, but the height of the peak proportion infected is lower than in the uniform scenario, regardless of whether migration between patches occurs or not. However, migration dramatically affects the rate at which herd immunity builds up in the population, as measured by the proportion of recovered individuals. Whilst without migration, the proportion infected declines at a similar rate to that at which it increased, with migration, herd immunity builds up much more slowly as infected individuals migrate to patches with low or absent herd immunity and cause small localized

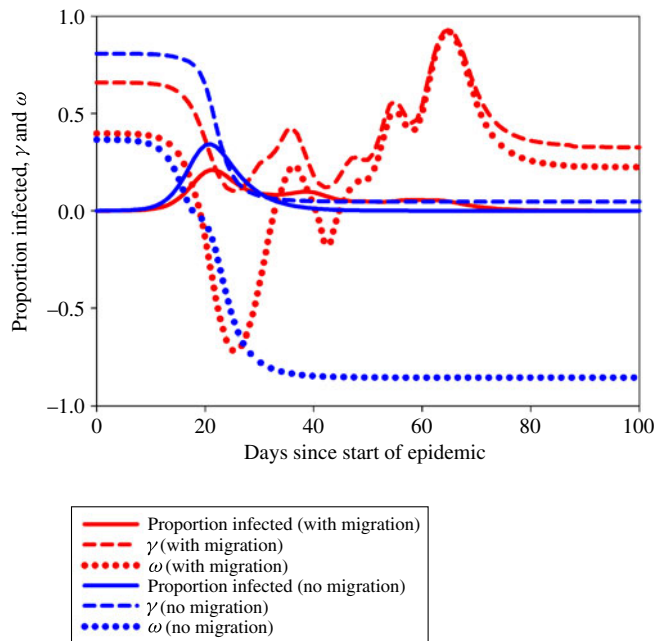


FIGURE 3. Changes in the correlation between infected and susceptible individuals, as expressed by values of  $\gamma$  and  $\omega$ , over the course of an epidemic in a patchy population with and without migration. The proportion of the population infected is shown with (red solid line) and without (blue solid line) migration as a reference. The red and blue dashed lines show  $\gamma$  over the course of an epidemic in a patchy population with and without migration, and the red and blue dotted lines show  $\omega$  given the same assumptions. (Colour available online.)

epidemics, reflected in the periodic peaks occurring in the tail of the epidemic curve. Whilst the initially periodic nature of the solution means that it takes a longer time for the peak level of herd immunity to be reached, eventually the system converges to a similar proportion recovered as in the uniform case. The proportion of the population immune at steady state in a patchy system without migration, however, is lower than in either a homogeneously (uniformly) mixing system, or one with migration.

The reasons for these differences are easily understood by analysis of the indices  $\gamma$  and  $\omega$ , which are shown in Figure 3. Visual inspection of changes in the  $\gamma$  indices shows that the strength of the relationship between the proportions infected and susceptible decreases as the epidemic curves reach their initial peaks, regardless of migration, as the proportion infected initially increases in patches seeded with infected individuals. After the epidemic peaks,  $\gamma$  behaves differently depending on whether migration occurs or not. Without migration, the epidemic declines monotonically towards extinction, but where migration occurs,  $\gamma$  periodically increases in value as epidemics fade out and decreases as others commence, driven by inter-patch movement. Inspection of the values of  $\omega$  assists in understanding where susceptibles and infectives are located in the patchy system, as well as their average numbers.



Where no migration occurs,  $\omega$  asymptotes above  $-1$ , which is interpreted as almost complete exclusion, that is, in any patches where there are infectives there are comparatively few susceptibles and vice versa [15]. Such an interpretation makes sense, as on inspection of the results in each patch, where infection has invaded a patch, infectives outnumber susceptibles by at least 100 to one, and in disease-free patches there are no infectives. One can see how  $\omega$  usefully tracks the change from a proportional relation of infectives to susceptibles at time zero to the eventual end of the epidemic. With migration,  $\omega$  initially declines similarly to the case with no migration, but then oscillates before approaching a steady state. The oscillations have decreasing amplitude as migration drives small localized epidemics until the proportion immune increases sufficiently to cause epidemic fade-out. The notable peak value of  $\omega$  occurring at approximately 65 days is interpreted biologically as the point at which a higher proportion of individuals are infected than susceptible. After this point the proportion recovered increases rapidly, as reflected in the rapid decay in the value of  $\omega$  after 70 days. Note that  $\omega$  never becomes negative after this final peak, but remains positive because, unlike in the case with no migration, where patches are either disease free or have more susceptibles than infectives, with migration all patches tend towards a theoretical final proportion recovered. This final proportion immune is generally predicted well by the solution of the standard SIR model [19], and thus the final proportion recovered is similar in the patchy case with migration and in the homogeneous-mixing case (see Figure 2).

In summary, for short-lived diseases such as influenza, migration and patchiness make little impact on the timing of the epidemic peak but have a strong effect on the aftermath of an epidemic. Where no migration occurs between patches, the epidemic curve declines monotonically and the final total proportion infected is greater than in the homogeneous case. In contrast, where migration occurs between patches after epidemic commencement, an epidemic lasts much longer and its decline is characterized by periodic smaller epidemics driven by inter-patch movement of infectives. The final total proportion of infectives is similar to the homogeneous case.

**3.3. Example 2: a long-lived sexually transmitted infection** Whereas the respiratory agent modelled has an infection duration of days, the infectious period of some sexually transmitted infections can last for a year or more [7]. Therefore, an epidemic of a human papillomavirus-like (HPV) sexually transmitted infection was simulated over a 5-year period ( $R_0$  approximately 1.5, recovery rate of 0.8 per annum). Individuals were assumed to move between patches at the same rate as in the short-lived infection model, namely one randomly selected individual per patch per day moved to an adjacent patch. In contrast to a previous paper by Waters [26], which also looked at the effect of patchy populations on HPV dynamics, here it was assumed that individuals leaving the infected state enter an immune state rather than becoming susceptible once more.

Some similar effects of migration on the build-up of immunity as in shorter-lived epidemics can be observed by analysis using the  $\gamma$  and  $\omega$  indices (see Figure 4).

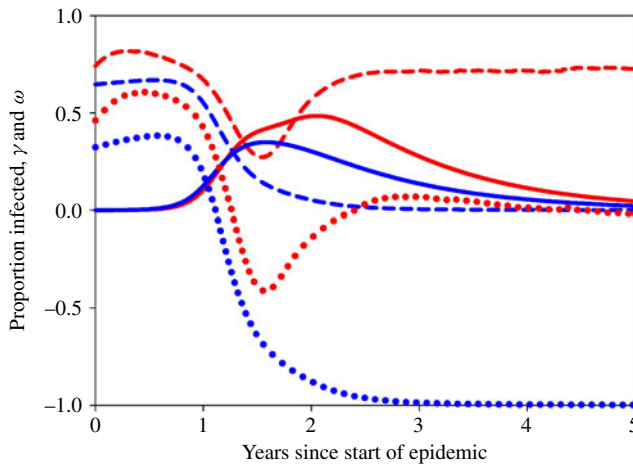


FIGURE 4. Changes in the correlation between infected and susceptible individuals, as expressed by values of  $\gamma$  and  $\omega$ , over the course of an epidemic that unfolds over several years. Lines of a given type and colour track the proportion infected or recovered under scenarios whose assumptions correspond to those yielding lines of the same colour and type in Figure 3. (Colour available online.)

Namely, in a patchy system without migration, disease-free patches may persist, resulting in incomplete disease spread and a lower level of herd immunity, but when migration occurs, all patches tend towards the theoretical final proportion recovered as infectives migrate to all patches. However, some features of this more slowly developing epidemic differ in important ways from the shorter-term infection described above. In the short-lived respiratory infection, the peak proportion infected but not the time taken for the epidemic to peak changed with patchiness and migration; additionally, migration resulted in a longer epidemic duration and contributed periodicity to the declining epidemic curve. In contrast, in the long-lived infection both the time taken to reach the epidemic peak and the peak proportion infected were affected by migration and patchiness, but the monotonic character of the epidemic fade-out and the proportion infected at the peak did not change, and there was no evidence of periodicity in the tail of the epidemic curve (compare Figure 5 to Figure 2). Most importantly, the epidemic peak occurred earlier and the epidemic died out sooner in a patchy system with no migration. When migration occurred in a patchy system, the epidemic peaked approximately six months sooner than in the homogeneous model, and the epidemic died out sooner. The effect of migration on peak size and duration therefore lessens as infection duration increases.

In summary, migration and patchiness have different effects depending on the length of the infectious period. For short-lived infections, the time for the epidemic to peak is not affected by migration or patchiness, but as the duration of the infectious period increases, the epidemic peak occurs earlier in more discrete environments. The fully discrete system modelled (patchy habitat, with some disease-free patches, and no

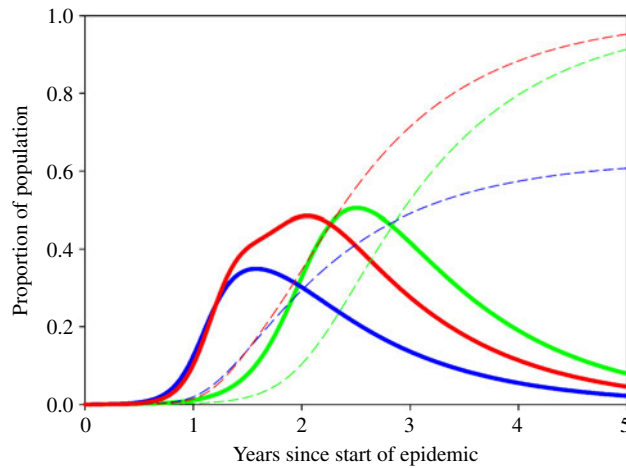


FIGURE 5. The proportion of the population infected and recovered during an epidemic that unfolds over several years. Lines of a given type and colour track the proportion infected or recovered under scenarios whose assumptions correspond to those yielding lines of the same type and colour in Figure 2. (Colour available online.)

movement between patches) therefore had the most rapid epidemic peak for long-lived epidemics, and also the quickest epidemic fade-out. This contrasts with the short-lived epidemic, where patchiness alone did not affect the speed of epidemic fade-out, but migration between patches resulted in an epidemic of longer duration. In the long-lived disease model, epidemics in patchy environments with migration still faded out more rapidly than those in homogeneously mixing populations.

#### 4. Discussion and conclusions

The models presented are phenomenological in character, and therefore are not truly representative of what actually occurs in nature, but nevertheless yield qualitative insights into the effects of patchiness and of migration between patches on the development of two very different types of infections. It is apparent that Lloyd's index of interspecific mean crowding appears within the transmission term of the basic SIR model; this renders analysis of the SIR model in terms of spatial changes in the numbers of infectives and recovered using tools based on the mean crowding index possible. Whilst Iwao's index  $\gamma$  yields limited qualitative information, being restricted to graphically representing the strength of the proportional relationship between numbers of susceptibles and infectives, the  $\omega$  index yields valuable insights into exactly how the spatial dynamics of a patchy system with migration differ from those of one without migration. Importantly,  $\omega$  can be used to understand graphically why patchiness and migration can result in very different dynamics for an epidemic caused by a virulent agent with a short duration of infection compared to one with

a long duration of infection. Future work may include incorporating phenomena such as variable transmission rates within patches, age or sex stratified populations, variable migration rates between different patches, and different migration parameters for infectives and susceptibles.

The use of  $\gamma$  and  $\omega$  as an analysis technique to understand the likely distribution of  $S$  and  $I$  across patches distinguishes this paper from other papers examining patchy SIR models. Arino et al. [3, 4] studied the dynamics of SEIR models in patchy habitats with migration independent of disease status (as in this paper) and with migration determined by disease status. On the whole, the results of this paper support those of Arino et al. in that the infections modelled tend towards an equilibrium with disease present in each patch [4]. Fulford et al. [11] used metapopulation models to investigate the dynamics of sexually transmitted bovine tuberculosis in possums. Whilst the circular stepping stone model employed here has some similarities with the loop network structure used for some of the possum metapopulations, direct comparison of the results is not possible because there was no recovered state in the possum model, and many of our results relate to the importance of patchiness and migration to the development of herd immunity. Fulford et al. did find, however, that in a loop or circular network the basic reproductive number of the disease stays constant regardless of the number of patches employed, indicating that the results in this paper would not be changed by increasing or reducing the number of patches used in the simulations.

With a short-lived infectious agent, patchy systems with migration have longer epidemic durations, but reach almost the same herd immunity level as the homogeneous case at equilibrium. Neither patchiness nor migration affect the timing of the peak proportion infected during a short-lived epidemic. In contrast, for long-lived epidemics, both migration and patchiness reduce rather than increase epidemic duration, and may also increase the peak proportion infected. Graphical analysis using the  $\omega$  index shows that for both short- and long-lived epidemics, the equilibrium solutions of patchy models with migration are similar to those for homogeneous systems. When either short- or long-lived epidemics begin in patchy systems without migration, however, the proportion immune at post-epidemic equilibrium is lower than in patchy systems with migration or the homogeneous model. This demonstrates that migration is still crucial to the development of herd immunity in a patchy environment even though it does not drive an increased epidemic duration for long-lived infectious agents.

Overall, this paper illustrates that when managing epidemics caused by highly virulent infections, controlling the movement of persons who may be infected is a two-edged sword. Inhibition of movement may lead to a shorter epidemic duration, but may inhibit the build-up of herd immunity, potentially leading to additional epidemic waves in the future. For a non-life-threatening infection, it may be better to treat symptoms than to inhibit movement, for as was shown in the recent 2009 influenza pandemic, adults infected with more mild strains in their youth or childhood were less susceptible to related pandemic strains [16].

## References

- [1] R. M. Anderson and R. M. May, *Infectious diseases of humans: dynamics and control* (Oxford University Press, Oxford, 1991).
- [2] Anonymous, “Influenza in a boarding school”, *Br. Med. J.* **1** (1978) 586; doi:10.1136/bmj.1.6112.586.
- [3] J. Arino, J. R. Davis, D. Hartley, R. Jordan, J. M. Miller and P. van den Driessche, “A multi-species epidemic model with spatial dynamics”, *Math. Med. Biol.* **22** (2005) 129–142; doi:10.1093/imammb/dqi003.
- [4] J. Arino and P. van den Driessche, “Metapopulations epidemic models. a survey”, in: *Nonlinear dynamics and evolution equations*, Volume 48 of *Fields Inst. Commun.* (eds H. Brunner et al.), (American Mathematical Society, Providence, RI, 2006), 1–12.
- [5] N. D. Barlow, “A spatially aggregated disease/host model for bovine Tb in New Zealand possum populations”, *J. Appl. Ecol.* **28** (1991) 777–793; doi:10.2307/2404207.
- [6] M. S. Bartlett, “Measles periodicity and community size”, *J. R. Statist. Soc. Ser. A* **120** (1957) 48–70; doi:10.2307/2342553.
- [7] K. Begg et al., “Australia’s notifiable diseases status, 2006: annual report of the national notifiable diseases surveillance system—results: sexually transmissible diseases”, *Commun. Dis. Intell.* **32** (2008) 139–208.
- [8] N. Bez, “On the use of Lloyd’s index of patchiness”, *Fisheries Oceanography* **9** (2000) 372–376; doi:10.1046/j.1365-2419.2000.00148.x.
- [9] J. A. Downing, “Spatial heterogeneity: evolved behaviour or mathematical artefact?”, *Nature* **323** (1986) 255–257; doi:10.1038/323255a0.
- [10] K. Fujita, “A new method for describing predator–prey relations in discontinuous environments”, *Res. Popul. Ecol.* **26** (1984) 379–388; doi:10.1007/BF02515501.
- [11] G. R. Fulford, M. G. Roberts and J. A. P. Heesterbeek, “The metapopulation dynamics of an infectious disease: tuberculosis in possums”, *Theor. Popul. Biol.* **61** (2002) 15–29; doi:10.1006/tpbi.2001.1553.
- [12] G. P. Garnett, J. Swinton, R. C. Brunham and R. M. Anderson, “Gonococcal infection, infertility, and population growth: II. The influence of heterogeneity in sexual behaviour”, *Math. Med. Biol.* **9** (1992) 127–144; doi:10.1093/imammb/9.2.127.
- [13] S. Iwao, “A new regression method for analyzing the aggregation pattern of animal populations”, *Res. Popul. Ecol.* **10** (1968) 1–20; doi:10.1007/BF02514729.
- [14] S. Iwao, “A note on the related concepts ‘mean crowding’ and ‘mean concentration’”, *Res. Popul. Ecol.* **17** (1976) 240–242; doi:10.1007/BF02530775.
- [15] S. Iwao, “Analysis of spatial association between two species based on the interspecies mean crowding”, *Res. Popul. Ecol.* **18** (1977) 243–260; doi:10.1007/BF02510851.
- [16] J. H. Jacobs et al., “Searching for sharp drops in the incidence of pandemic A/H1N1 influenza by single year of age”, *PLoS ONE* **7** (2012) e42328; doi:10.1371/journal.pone.0042328.
- [17] M. Kimura and G. H. Weiss, “The stepping stone model of population structure and the decrease of genetic correlation with distance”, *Genetics* **49** (1964) 561–576.
- [18] M. Lloyd, “Mean crowding”, *J. Animal Ecol.* **36** (1967) 1–30; doi:10.2307/3012.
- [19] J. Ma and D. J. D. Earn, “Generality of the final size formula for an epidemic of a newly invading infectious disease”, *Bull. Math. Biol.* **68** (2006) 679–702; doi:10.1007/s11538-005-9047-7.
- [20] T. Maruyama, “On the rate of decrease of heterozygosity in circular stepping stone models of populations”, *Theor. Popul. Biol.* **1** (1970) 101–119; doi:10.1016/0040-5809(70)90044-4.
- [21] J. Matthiopoulos, J. Harwood and L. Thomas, “Metapopulation consequences of site fidelity for colonially breeding mammals and birds”, *J. Animal Ecol.* **74** (2005) 716–727; doi:10.1111/j.1365-2656.2005.00970.x.
- [22] P. E. Parham and N. M. Ferguson, “Space and contact networks: capturing the locality of disease transmission”, *J. R. Soc. Interface* **3** (2006) 483–493; doi:10.1098/rsif.2005.0105.
- [23] R Core Team. *R: a language and environment for statistical computing*. R Foundation for Statistical Computing, Vienna, 2012.

- [24] G. E. Svendsen, “Behavioral and environmental factors in the spatial distribution and population dynamics of a yellow-bellied marmot population”, *Ecology* **55** (1974) 760–771; doi:10.2307/1934412.
- [25] K. M. E. Turner, E. J. Adams, N. Gay, A. C. Ghani, C. Mercer and W. J. Edmunds, “Developing a realistic sexual network model of chlamydia transmission in Britain”, *Theor. Biol. Med. Model.* **3** (2006); doi:10.1186/1742-4682-3-3.
- [26] E. K. Waters, “Aggregation and competitive exclusion: explaining the coexistence of Human *Papillomavirus* types and the effectiveness of limited vaccine conferred cross-immunity”, *Acta Biotheoretica* **60** (2012) 333–356; doi:10.1007/s10441-012-9161-5.